Spectrum in the strong turbulence region of Gross-Pitaevskii turbulence

Kyo Yoshida[1], Hideaki Miura[2], and Yoshiyuki Tsuji[3]
[1]Division of Physics, Faculty of Pure and Applied Sciences, University of Tsukuba, Tsukuba, Japan
[2]National Institute for Fusion Science, Toki, Japan
[3]Graduate School of Engineering, Nagoya University, Nagoya, Japan

This is a post-peer-review, pre-copyedit version of an article published in Journal of Low Temperature Physics. The final authenticated version is available online at: http://dx.doi.org/10.1007/s10909-019-02197-4 .

Abstract

Numerical simulations of the Gross-Pitaevskii equation which describes the dynamics of quantum fluids are performed focusing on scales larger than the healing length. Dissipation and pumping of the mass are applied in high and low wavenumber ranges, respectively, in order to achieve turbulent states. In this setting of dissipation and pumping, it is found that the mass, or the particle number, cascades from low to high wavenumbers and a constant flux of the particle number is observed in the cascading wavenumber range. The spectrum $F(k)$ (k is the wavenumber) of the order parameter field at the turbulent state is analyzed and it is found that the obtained $F(k)$ is consistent with the form $\propto k^{-1}[\ln(k/k_0)]^{-1}$ (k_0 is the lower-end wavenumber of the scaling range) which is derived from a closure approximation of the particle-number transfer range of strong turbulence [K. Yoshida, T. Arimitsu, Journal of Physics A:Mathematical and Theoretical **46**(33), 335501 (2013)].

1 Introduction

In a Bose gas or liquid, the order parameter $\psi(\vec{x},t) \in \mathrm{C}$, which is the expectation value of the field operator $\hat{\psi}(\vec{x},t)$, is nonzero for a temperature $T < T_c$ with T_c being some critical temperature. Under certain conditions[1], dynamics of the order parameter is approximately described by the Gross-Pitaevskii (GP) equation [2, 3],

$$\mathrm{i}\hbar\frac{\partial}{\partial t}\psi(\vec{x},t) = -\frac{\hbar^2}{2m}\nabla^2\psi(\vec{x},t) - \mu\,\psi(\vec{x},t) + g|\psi(\vec{x},t)|^2\psi(\vec{x},t), \tag{1}$$

where m is the mass of the boson, g is the coupling constant, μ is the chemical potential and $\hbar$ is the Planck constant divided by 2π. The chemical potential μ may be related to the particle number density field $n(\vec{x},t) := |\psi(\vec{x},t)|^2$ by $\mu = g\overline{n}$ where the bar denotes the spatial average. Let $\psi(\vec{x},t) = \sqrt{n(\vec{x},t)}\mathrm{e}^{\mathrm{i}\theta(\vec{x},t)}$ and then $n(\vec{x},t)$ and $\vec{v}(\vec{x},t) := (\hbar/m)\vec{\nabla}\theta(\vec{x},t)$, can be viewed as the density field and the velocity field, respectively, of a fluid. In this paper, we refer to the fluid as quantum fluid. Some examples of quantum fluids are the superfluid component in superfluid phase of ^{4}He and the Bose-Einstein condensates (BECs) of ultracold atoms.

The fluctuation part $\hat{\psi}(\vec{x},t) - \psi(\vec{x},t)$, which is neglected in the GP equation, may be weakly coupled to the system of the GP equation and may act as a particle and energy reservoir which causes dissipation of the particle number and the energy to the system of the GP equation, especially in small scales. See, e.g., Kobayashi and Tsubota[4] for a related theoretical and numerical study. Recently, Navon, Gaunt, Smith and Hadzibabic[7], and Tsatsos et al. [8] managed to inject energy into the BEC of ^{87}Rb atoms by stirring it with magnetic fields varying in the order of the system size. When quantum fluids are equipped with the dissipation at small scales and the external forcing at large scales, fluid motions may evolve into turbulence

in a similar manner as in the case of the classical fluids obeying the Navier-Stokes equation. There have been many experimental and numerical studies on the turbulent velocity fields of quantum fluids in relation with those of classical fluids. See, e.g., the reviews Refs. [5, 6] and the references cited therein.

In the studies of turbulence of quantum fluids, it is natural to focus not only on $\vec{v}(\vec{x},t)$ but also on $\psi(\vec{x},t)$ which is a more fundamental variable regarding the dynamics. The basic quantity which describes the statistics of $\psi(\vec{x},t)$ is the spectrum $F(k,t) := \sum_{k-1/2\le|\vec{k}'|<k+1/2} |\psi_{\vec{k}'}(t)|^2$, where $\psi_{\vec{k}}(t) := (2\pi)^{-3}\int_{\mathscr{D}} d\vec{x}\psi(\vec{x},t)$ $\exp(-\mathrm{i}\vec{k}\cdot\vec{x})$ is the Fourier transform, and $\mathscr{D}$ is the domain of the fluid which we set to be a three dimensional cube with the side length 2π and the periodic boundary conditions. When the contribution of the nonlinear term, the last term in the rhs of (1), is small, $F(k)$ (the time argument will be omitted hereafter) can be analyzed using the weak wave turbulence (WWT) theory [9, 10]. Dyachenko, Newell, Pushkarev, and Zakharov[11] derived $F(k) \propto k^{-1}[\ln(k/k_0)]^{-1/3}$ for the energy cascade range and $F(k) \propto k^{-1/3}$ for the particle-number cascade range, where k_0 is the lower-end wavenumber of the cascade range. For the case when the symmetry is broken, i.e. $\overline{\psi} \neq 0$, Fujimoto and Tsubota[12] derived $F(k) \propto k^{-7/2}$ using WWT theory and verified it with a numerical simulation of the GP turbulence.

As the scales of interest become larger, or the wavenumbers become smaller, the nonlinear term in Eq.(1) becomes more significant and the WWT theory is not applicable any more. We call such a scale region the strong turbulence region. Yoshida and Arimitsu analyzed the strong turbulence region of the GP turbulence by a spectral closure approximation[13]. It is derived that $F(k) \propto k^{-2}$ for the energy cascade range and $F(k) \propto k^{-1}[\ln(k/k_0)]^{-1}$ for the particle-number cascade range. It should be noted that the existence of the energy or particle-number cascade is the assumption of the analysis and that the conditions for the emergence of these cascades are not clear. Furthermore, closure approximations are, in general, empirical methods to analyze the system with strong non-linearity and they are not mathematically rigorous. Therefore, the results from the closure approximation in Ref. [13] should be verified by the numerical simulations or the experiments.

In this study, we perform numerical simulations of the GP equations focusing on large scales which correspond to the strong turbulence region. We apply dissipation and pumping of fluid mass, or particles, in high and low wavenumber ranges, respectively, expecting that some sort of cascade will emerge. The obtained spectrum $F(k)$ is compared with that derived from the closure approximation.

2 Set up of the numerical simulations

We performed numerical simulations of the GP equation equipped with external pumping and dissipation of the fluid mass. The basic setting of the simulation is same as that in Ref. [14]. The domain $\mathscr{D}$ of the fluid is a three dimensional cube with the side length 2π and periodic boundary conditions are applied. We use the units such that $\tau := \hbar/g\overline{n} = 1$ and $\overline{n} = 1$. The time evolution equation for $\psi_{\vec{k}}$ is given by

$$\frac{\partial}{\partial t}\psi_{\vec{k}} = -\mathrm{i}\xi^2 k^2 \psi_{\vec{k}} + \mathrm{i}\psi_{\vec{k}} - \mathrm{i}\sum_{\vec{k}+\vec{p}-\vec{q}-\vec{r}=\vec{0}} \psi^*_{\vec{p}}\psi_{\vec{q}}\psi_{\vec{r}} + D_{\vec{k}} + P_{\vec{k}}, \tag{2}$$

where $\xi := \hbar/\sqrt{2mg\overline{n}}$ is the healing length and $D_{\vec{k}}$ and $P_{\vec{k}}$ are the external dissipation and pumping of the fluid mass, respectively. For given $D_{\vec{k}}$, $P_{\vec{k}}$ and initial condition $\psi_{\vec{k}}(t=0)$, the time evolution of $\psi_{\vec{k}}(t)$ by Eq.(2) is simulated by using a fourth-order Runge-Kutta method with the time increment being denoted by Δt. For convolutions in the last term of the rhs of (2), we use an alias-free spectral method. Due to the dealiasing, the maximum wavenumber $k_{\max}$ resolved in the simulation is $k_{\max} = (2\sqrt{2}/3)N/2$, where N is the number of grid points along each of the coordinates in real space. The initial fields are given by $|\psi_{\vec{k}}| = Ak^2\exp(k^2/k_{\mathrm{i}}^2)$ with random phases, where the peak wavenumber k_{i} is set to 2 and A is a constant determined from the constraint $\overline{n} = 1$. Alternative initial fields are the resulting fields of a prior simulation with the above initial fields.

We employ a simple type of the dissipation and pumping acting on high and low wavenumber ranges (i.e. large and small scales), respectively, expecting that some general features of quantum fluid turbulence that are irrelevant to the specific type of dissipation and pumping will appear in the intermediate wavenumber range, if dissipation and forcing wavenumber ranges are sufficiently separated. We use a Laplacian type model, $D_{\vec{k}} = -\nu k^2 \psi_{\vec{k}}$, for the dissipation and the pumping is introduced by amplifying low-wavenumber

Table 1: Parameters in the simulations. ξ is the healing length, ν the coefficient of the dissipation term, $k_{\rm p}$ the bottom wavenumber of the pumping range, N number of grid points along one of the coordinate direction, $k_{\rm max}$ maximum wavenumber resolved, Δt the time increment and the particle-number dissipation rate $\varepsilon_{\rm n}$. All the values are given in the unit such that $\tau := \hbar/g\overline{n} = 1$, $\Delta k := 2\pi/L = 1$ and $\overline{n} = 1$.

	$\xi[\times 10^{-3}]$	$\nu[\times 10^{-3}]$	$k_{\rm p}$	N	$k_{\rm max}$	Δt	$\varepsilon_{\rm n}$
RUN1	0.03125	0.016	2.5	1024	483	0.01	0.185
RUN2	0.03125	0.008	2.5	1024	483	0.01	0.190
RUN3	0.03125	0.004	2.5	2048	965	0.01	0.176
RUN4	0.03125	0.002	2.5	2048	965	0.01	0.179
RUN5	0.125	0.002	2.5	2048	965	0.01	0.179
RUN6	0.5	0.002	2.5	2048	965	0.01	0.178

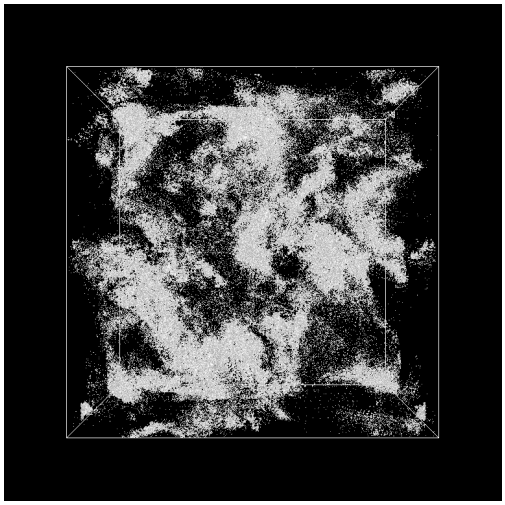

Figure 1: Density isosurfaces at a low density $n = 0.004\overline{n}$ in the whole cube domain. The side length of the cube is 2π and the healing length $\xi = 0.5 \times 10^{-3}$ (RUN6). The visualization data are produced by using VISMO[15].

modes as $P_{\vec{k}} = \alpha\psi_{\vec{k}}(0 < |\vec{k}| < k_{\rm p})$ and $P_{\vec{k}} = 0(|\vec{k}| = 0, |\vec{k}| \geq k_{\rm p})$, where $k_{\rm p}$ is the bottom wavenumber of the pumping range and the parameter α is determined at every time step so as to compensate the loss of mass due to the dissipation, i.e., $\overline{n}$ is kept at 1.

The values of the parameters used in the present simulations are listed in Table 1. The six simulated time sequences are named RUN1 – 6 and they are simulated up to a time at which the spectrum $F(k)$ is quasi stationary. Since we are interested in strong turbulence regions, we set $k_{\rm max}\xi \leq 1$, i.e., length scales larger than ξ are resolved in the simulations.

3 Structure of the density field

Throughout RUN1 – RUN6, we observed $|\overline{\psi}|^2/\overline{n} < 10^{-3}$, which implies that the spatial mean $\overline{\psi}$ scarcely emerged and that the symmetry with respect to the global phase shift $\psi(\vec{x}) \to \psi(\vec{x})e^{i\Theta}$ is scarcely broken. The three dimensional structure of low density regions are displayed in Fig. 1. The figure shows isosurfaces at $n(\vec{x}) = 0.004\overline{n}$ and quantized vortex lines, specified by $n = 0$, should be surrounded by the surfaces. It can be seen that vortices are not distributed uniformly in space and form clusters in a length scale which is comparable with the system size. The cluster structure may be analogous to that of intense vorticity regions observed in numerical simulations of turbulence obeying the Navier-Stokes equation[16]. Note that we put $k_{\rm max}\xi = 0.483$ so that the healing length ξ, which is the typical length scale of the density variation around

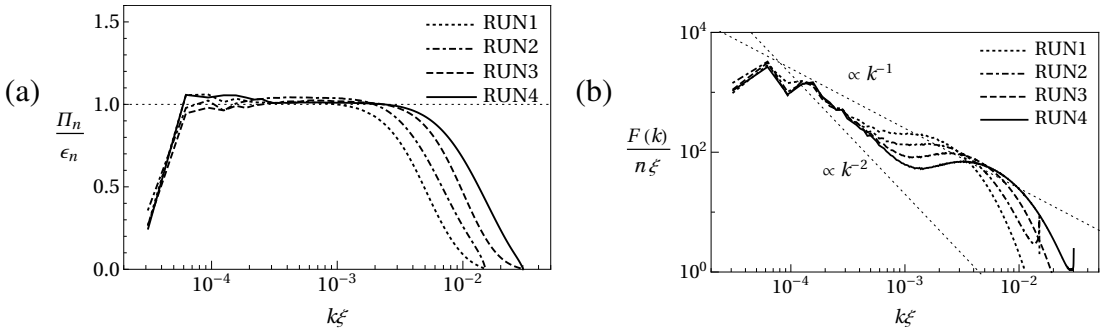

Figure 2: (a) Particle-number flux $\Pi_{\rm n}(k)$ normalized by the particle-number dissipation rate $\varepsilon_{\rm n}$ for the healing length $\xi = 0.3125 \times 10^{-4}$ and several values of the particle-dissipation coefficient ν (RUN1 – 4). (b) Spectrum $F(k)$ for RUN1 – 4. Slopes of the dotted lines indicate $\propto k^{-1}$ and $\propto k^{-2}$.

the vortex lines, is not sufficiently resolved and therefore the structures of the individual vortices are not well captured. However, we expect that the large-scale structure of clustering observed in Fig. 1 reflects the general features of the GP strong turbulence. The expectation will be partially supported by the analysis in the next section, in which the spectrum $F(k)$ obtained in the simulation shows a general scaling law in the low wavenumber range.

4 Analysis of the spectrum $F(k)$

The particle number flux $\Pi_{\rm n}(k)$ through a wavenumber k can be given by $\Pi_{\rm n}(k) = -(\partial/\partial t)|_{\nu=0,\alpha=0} \sum_{\vec{k}'(k'\le k)} |\psi_{\vec{k}'}|^2$, where $(\partial/\partial t)|_{\nu=0,\alpha=0}$ denotes the contribution of the pure GP equation, i.e., without dissipation and pumping, to the time derivative. The particle-number flux $\Pi_{\rm n}(k)$ normalized by the particle-number dissipation rate $\varepsilon_{\rm n} = 2\nu \sum_{\vec{k}} k^2 |\psi_{\vec{k}}|^2$ is shown for fixed $\xi = 0.3125 \times 10^{-4}$ and several values of ν (RUN1 – 4) in Fig. 2a. It can be seen that there exists a range where $\Pi_{\rm n}(k)$ is approximately a constant $\varepsilon_{\rm n}(> 0)$. The lower-end wavenumber of the flux-constant range is $k\xi \sim 3 \times 10^{-4}$ and the higher-end wavenumber increases from $k\xi \sim 10^{-3}$ to 3×10^{-3} with the decrease of the dissipation coefficient ν. The energy flux $\Pi(k)$ can be also computed from the simulation data. But, it is found that $\Pi(k)$ depends on k and can not be approximated by a constant (the figure omitted). Thus, we conclude that the particle-number cascade from low to high wavenumber range occurs in the present setting of the GP turbulence.

The spectra $F(k)$ obtained from the same data (RUN1 – 4) are shown in Fig. 2b. The slope of the spectrum in the wavenumber range where the particle-number flux is approximately constant is between $F(k) \propto k^{-1}$ and $\propto k^{-2}$. However, there exists a bump around the higher end of the constant flux range and the width of the power law range is shortened due to the bump. The bump can be interpreted as the pileup of particles at the end of the constant flux range before the dissipation. The bump is also observed in the Navier-Stokes turbulence [17], but the bump in the GP strong turbulence seems to be more significant than that of the Navier-Stokes turbulence. Note that the slopes between $F(k) \propto k^{-1}$ and $\propto k^{-2}$ are also obtained in the numerical simulations of the GP equation with dissipation and pumping by Proment, Nazarenko and Onorato [18]. In comparison with Ref. [18], the typical wavenumbers, $k\xi \sim 10^{-4}$, in the scaling range of the present simulation is smaller and so that it is expected that the nature of the strong turbulence is more significantly reflected in the present simulation.

According to Ref.[13], $F(k)$ in the particle-number transfer range of strong turbulence is given by

$$F(k) \sim C_3 \Pi_{\rm n}^{1/2} k^{-1} \left[\ln\left(\frac{k}{k_0}\right) \right]^{-1} \quad (k_0 < k \ll k_1), \tag{3}$$

where the logarithmic correction near the lower-end wavenumber k_0 is applied and C_3 is a universal constant. Since the exponent -1 of the logarithmic term is marginal, a further correction may be required. However, we neglect it for it would be quite difficult to detect the further corrections in the present simulations with a limited width of the scaling range. The logarithmic correction near higher-end wavenumber

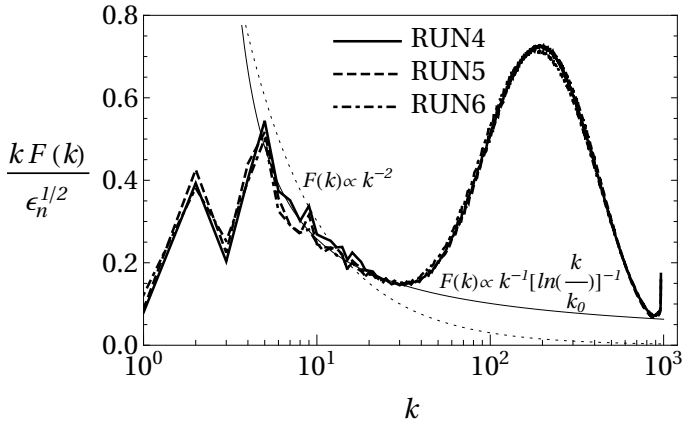

Figure 3: Compensated spectrum $kF(k)$ normalized by $\varepsilon_{\rm n}^{1/2}$ for the particle-dissipation coefficient $\nu = 0.2\times10^{-2}$ and several values of the healing length ξ (RUN4 – 6). Here, $\varepsilon_{\rm n}$ is the particle-number dissipation rate. Thin solid and dotted lines are fits to the data in the range $6 \le k \le 25$ with $F(k) = C_3 k^{-1}[\ln(k/k_0)]^{-1}$ and $F(k) = C'k^{-2}$, respectively.

k_1 is also neglected. This is because the cascade range where $\Pi_{\rm n}(k) \sim \varepsilon_{\rm n}$ holds is not very wide and the direct effect of the dissipation term $D_{\vec{k}}$ can not be neglected near k_1. In Fig.3, the compensated spectrum $kF(k)/\varepsilon_{\rm n}^{1/2}$ is given for fixed ν and several values of ξ (RUN4 – 6). We find that $F(k)$ is insensitive to ξ in the range of $0.3125\times10^{-4} \le \xi \le 0.5\times10^{-3}$, which is consistent with the scaling given in Eq. (3). Furthermore, Fig. 3 shows that Eq.(3) gives a better fit to the simulation data of $F(k)$ in a range $6 \le k \le 25$ in comparison with $F(k) = C'k^{-2}$. However, note that Eq.(3) has two fitting parameters C_3 and k_0, whereas $F(k) = C'k^{-2}$ has only one.

5 Discussion

In WWT, the energy and the particle number are both of second order in ψ and it can be easily argued that the energy (particle number) cascades in the forward (inverse) direction (See, e.g., Chap. 2 of Ref.[10]). In the strong turbulence, the interaction energy, which is of fourth order in ψ, is dominant and then the existences and directions of the cascades of multiple conservative quantities can not be argued as simply as in WWT.

In the present numerical simulations of the GP strong turbulence, we found that the forward cascade of particle number emerges when dissipation of fluid mass in a high wavenumber range and pumping in a low wavenumber range is applied. The obtained spectrum $F(k)$ is consistent with $F(k) \sim C_3\Pi_n^{1/2}k^{-1}[\ln(k/k_0)]^{-1}$ derived from a closure approximation for the particle-number transfer range of strong turbulence in Ref. [13]. The energy cascade in the strong turbulence is also assumed to exist in Ref. [13], but is not observed at least in the present setting of the simulation. The existence of the energy cascade in the GP strong turbulence is still an open question.

The relevance of the present setting of dissipation and pumping to existing experiments of stirred BEC turbulence is not clear at present. Navon, Gaunt, Smith and Hadzibabic[7] and Tsatsos et al. [8] obtained results which correspond to $F(k) \propto k^{-3/2}$ and $F(k) \propto k^{-2}$, respectively, in their experiments. The exponents $-3/2$ and -2 are comparable with the spectrum obtained in Fig. 2b, however the wavenumber range in their experiments are $k\xi \sim 1$ and in the present study $k\xi \ll 1$. It would be an interesting future study to obtain the comprehensive understanding of $F(k)$ in the whole scale range of both weak wave and strong GP turbulences by integrating the means of theoretical analyses, numerical simulations and experiments.

acknowledgements

This work was performed on "Plasma Simulator" (FUJITSU FX100) of NIFS with the support and under the auspices of the NIFS Collaboration Research programs (NIFS15KNSS064, NIFS18KNSS106). Development of some numerical codes used in this work was supported in part by the "Code development support program" of Numerical Simulation Reactor Research Project (NSRP), NIFS. The authors are grateful to N. Ohno and H. Ontani for the permission to use the visualization tool VISMO in this work.

References

[1] L. Pitaevskii, S. Stringari, *Bose-Einstein condensation* (Oxford University Press, 2003)

[2] L. Pitaevskii, Soviet Phys. JETP **13**, 451 (1961)

[3] E. Gross, J. Math. Phys. **4**, 195 (1963)

[4] M. Kobayashi, M. Tsubota, Phys. Rev. Lett. **97**, 145301 (2006)

[5] C.F. Barenghi, L. Skrbek, K.P. Sreenivasan, Proc. Natl. Acad. Sci. USA **111**, 4647 (2014)

[6] M. Tsubota, K. Fujimoto, S. Yui, J. Low Temp. Phys. **188**, 119 (2017)

[7] N. Navon, L. Gaunt, Alexander, R.P. Smith, Z. Hadzibabic, Nature **539**, 72 (2016)

[8] M.C. Tsatsos et al., Physics Reports **622**, 1 (2016)

[9] V.E. Zakharov, V.S. L'vov, G. Falkovich, *Kolmogorov Spectra of Turbulence I: Wave Turbulence* Springer, Berlin (1992)

[10] S. Nazarenko, *Wave Turbulence*, Lecture Notes in Physics **825**, Springer, Berlin (2011)

[11] S. Dyachenko, A. Newell, A. Pushkarev, V. Zakharov, Physica D **57**, 96 (1992)

[12] K. Fujimoto, M. Tsubota, Physical Review A **91**, 053620 (2015)

[13] K. Yoshida, T. Arimitsu, Journal of Physics A:Mathematical and Theoretical **46**(33), 335501 (2013)

[14] K. Yoshida, T. Arimitsu, J. Low Temp. Phys. **145(1-4)**, 219 (2006)

[15] N. Ohno, H. Ohtani, Plasma and Fusion Research **9**, 3401071 (2014)

[16] Y. Kaneda, T. Ishihara, J. Turbulence **7**(20), 1 (2006)

[17] Y. Kaneda et al, Phys. Fluids **15**, L21 (2003)

[18] D. Proment, S. Nazarenko, M. Onorato, Phys. Rev. A **80**, 051603(R) (2009)